Scheduling Based on Maximum PF Selection with Contiguity Constraint for SC-FDMA in LTE Uplink*

HONGSUK KIM[1], MIN YOUNG CHUNG[2], TAE-JIN LEE[2] MIHUI KIM[3]
AND HYUNSEUNG CHOO[2]
[1]*Advanced Communications Technology (ACT) R&D Lab of LG Electronic*
Seocho-gu, Seoul, Korea
[2]*College of Information and Communication Engineering, Sungkyunkwan University*
Suwon-si, Gyeonggi-do, Korea
[3]*Department of Computer & Web Information Engineering, Hankyong National University*
Anseong-si, Gyeonggi-do, Korea

E-mail: hassium.kim@gmail.com[1], {mychung; tjlee; choo}@ece.skku.ac.kr[2], mhkim@hknu.ac.kr[3]

Single-carrier frequency division multiple access (SC-FDMA), which is similar to multi carrier modulation type with orthogonal frequency domain multiple access (OFDMA), has been used as long term evolution (LTE) uplink access method due to its low PAPR and high UE power efficiency. SC-FDMA, however, has a constraint that subcarriers must be consecutively allocated to each user for every time slot due to the single carrier feature of the access type. This paper proposes an LTE uplink scheduling algorithm satisfying the contiguity constraint of resource allocation and ensuring high cell (system) throughput and fairness with low complexity. The proposed scheme, named MSCC, preferentially considers allocation to RBs based on the highest Proportional Fair scheduling metric in each physical resource block (RB) with the contiguity constraint. As a result of simulation analysis, MSCC has better fairness and cell throughput than the previous schemes (*i.e.*, RME, IRME algorithm) by 10% and 17% at most, respectively. We also analyze cell edge user throughput (the gathering with the cell users who have 5% lowest throughput) and PAPR. In the appendix, complexity analysis shows that the time complexity of the MSCC is better than the previous schemes.

Keywords: long term evolution (LTE), uplink, frequency domain packet scheduling (FDPS), resource allocation, single-carrier FDMA (SC-FDMA)

1. INTRODUCTION

Recently, the increase in data request for mobile devices has caused several problems in processing enormous amount of radio resources. The 3rd generation partnership project (3GPP) uses long term evolution (LTE) to solve these problems. The 3GPP Release 8 (Rel-8) Long Term Evolution (LTE) wireless broadband standard has gained considerable attention from the telecommunication industry recently because of its capability of providing faster mobile broadband services and simpler QoS management [1]. Orthogonal frequency domain multiple access (OFDMA) is used in the LTE downlink, and single-carrier frequency division multiple access (SC-FDMA) is used in the LTE uplink. OFDMA is powerful for multipath fading and has high frequency efficiency and scalability. However, OFDMA causes a power problem for mobile devices by high

Received; revised ; accepted
Communicated by Hyunseung Choo.
* This work was partly supported by the ICT R&D program of MSIP/IITP [10041244, Smart TV 2.0], [IITP-14-911-05-006, Development of Core Technology for Autonomous Network Control and Management] and Basic Science Research Program through NRF of Korea, funded by MOE(NRF-2010-0020210)

peak-to-average power ratio (PAPR); even at one of the OFDM symbols, if RF power changes suddenly, then the PAPR increases. SC-FDMA is used in the LTE uplink, because it not only provides multiple accesses but also has a single-carrier characteristic [2-3].

In operating LTE frequency resource allocation, twelve subcarriers are chained to one physical resource block (RB). SC-FDMA and OFDMA consider channel states and use frequency domain packet scheduling (FDPS) to allocate RBs, parts of system frequency resources, to each user. In particular, SC-FDMA requests a localized allocation (LFDMA) to maintain a low PAPR, and thereby has a constraint that RBs allocated to each user have to be consecutive [4-6]. With the contiguity constraint, the uplink resource allocation uses channel-aware scheduling, in which high multi-user diversity gain is feasible. The uplink scheduling is performed based on scheduling metrics made by the signal to interference and noise ratio (SINR) for each user. In this paper, uplink scheduling adopts a proportionally fair (PF) scheduling metric to guarantee a level of fairness [7].

As stated previously, in LTE uplink resource allocation, RB has to be allocated consecutively to one user in every time slot to maintain the single-carrier characteristic. Three scheduling techniques have been suggested to expand to neighbor RBs by the highest PF metric of users [8]. Recursive maximum expansion (RME) was the superior algorithm among the three algorithms. The RME algorithm expanded resource allocation to neighbor RB with the highest PF metric. However, the RME is inefficient in terms of the throughput because it always expands allocation to neighbors and does not consider alternative allocation paths. The performance of the RME is compared with some LTE uplink scheduling algorithms for both channel dependent and proportional fairness paradigms in Safa H et al [9]. Improved recursive maximum expansion (IRME) is proposed to make up for the weakness in the RME algorithm [10]. However, the IRME still has a shortcoming of flexible resources allocation with higher complexity and lower fairness than the RME.

In this paper, we propose a new scheduling algorithm that increases the system throughput with low complexity, and guarantees better fairness than in previous scheduling algorithms, while keeping the constraint that RB should be allocated consecutively in the frequency domain. The proposed scheme through maximum PF selection with contiguity constraint (MSCC) decides whether to allocate resources with the contiguity constraint after searching for the highest metric in each RB. The MSCC operates more simply and has a higher throughput than previous schemes that allocate resources by expanding to neighbors. In addition, the MSCC considers the highest PF metric in each RB so that it has the ability to schedule flexibly when the number of users changes suddenly. The complexity of MSCC is reduced compared to those of the RME and the IRME. The simulation analyzes the system throughput of each scheme. The MSCC achieves better performance than previous schemes in terms of throughput and fairness. It improves the fairness by at most 10% and the throughput by at most 17%.

The remainder of this paper is organized as follows. Section 2 refers to the basic FDPS and describes the previous scheduling algorithms, the conventional RME and the IRME, with simple examples. Section 3 explains the operating steps of the MSCC and details its advantages. Section 4 shows the simulation results for fairness, system throughput, cell edge user throughput, and PAPR. Finally, we conclude the paper with

Section 5 and provide complexity analysis in the appendix.

2. RELATED WORK

2.1 Frequency Domain Packet Scheduling System

The LTE uplink FDPS uses the channel gain estimated from every user in the frequency domain as an input for scheduling. Each user sends a sounding reference signal (SRS) to a scheduling node (*i.e.*, eNodeB), and the SRS is used as a channel quality indicator (CQI). CQI information keeps being updated for every transmission time interval (TTI) at the scheduling node. The FDPS scheduler decides the total number of users and RBs using this CQI information and hybrid automatic retransmit request (HARQ), which figures out the number of users who need to retransmit [11]. An RB is made up of 12 subcarriers. User location and channel state of each subcarrier are important factors to consider for scheduling. In this paper, we use the PF algorithm with a scheduling metric value calculated from the RB value of each user. The PF algorithm is an essential component to prevent the unfair allocation of most of the resources to just a few users who have good channel conditions. It takes fairness and throughput into consideration by appropriately allocating resources to all users [12-14].

	RB1	RB2	…	RBK
UE1	$m_{1,1}$	$m_{1,2}$	…	$m_{1,K}$
UE2	$m_{2,1}$			$m_{2,K}$
⋮	⋮			
UEN	$m_{N,1}$	$m_{N,2}$	…	$m_{N,K}$

Fig. 1. Input metric M.

Fig. 1 shows a two-dimensional array **M** composed of PF metrics generated by users and RBs for every time slot. **M** has N rows and K columns (*i.e.*, [N×K]). M is presented as $(m_{n,k})_{N\times K}$, where $m_{n,k}$ is a PF metric of user n and RB k (*i.e.*, $\mathbf{M}=(m_{n,k})_{N\times K}$, $1 \leqslant n \leqslant N$, $1 \leqslant k \leqslant K$). The FDPS scheduler consequently aims to allocate resources to satisfy the following mathematical equation (1) for every time slot with input values in Fig.1 [15-17].

$$M_{sum} = \max \sum_{n=1}^{N} \sum_{k=1}^{K} m_{n,k} a_{n,k} \tag{1}$$

$$A = (a_{n,k})_{N\times K}, \quad a_{n,k} \in \{0, 1\}, \quad \sum_{n=1}^{N} \sum_{k=1}^{K} a_{n,k} = K, \quad \forall k : \sum_{n=1}^{N} a_{n,k} = 1 \tag{2}$$

where $a_{n,k}$ denotes an indicator that has a 0 or 1 value and represents whether RB k is

allocated to user n or not (*i.e.*, equation (2)). In the next subsection, we introduce existing scheduling algorithms for FDPS in SC-FDMA based on the M_{sum} equation.

2.2 Conventional RME & Improved RME (IRME) Algorithms

Recursive Maximum Expansion: This algorithm expands resource allocation to neighbor RB after the frequency domain scheduler selects the highest metric in the multi-dimensional array consisting of input PF metrics. The RME is scheduled by the following procedure. First, the scheduler determines UE and RB that have the highest PF metric and allocates it. The scheduler checks if the both-side neighbor's metrics are the highest among all metrics in each RB; if so, it does the allocation. Resource allocation is continuously performed until another UE that has a higher metric value than the first UE in the same RB appears. The allocated UE (row) and RBs (columns) are ruled out in the array. These steps are repeated to allocate resources to all UEs. If all UEs get resource blocks, but all RBs are not fully used for resource allocation, the allocations for unused RBs are considered by the UE that has the highest metric with the contiguity constraint among the allocated metrics of both-side UEs [8]. In the appendix, we describe the complexity of the RME algorithm.

Improved RME: This algorithm is an improved version of the RME (IRME) scheme from the viewpoint of cell throughput. The IRME schedules more flexible resource allocation paths than the RME algorithm through a ranking threshold (*Tr* value). The value *Tr* denotes the number of resource allocation paths. In other words, the IRME considers resource allocation paths with the *Tr* value from the highest metric to the *r*-th highest metric in a neighbor's RB. The procedure of the IRME is as follows. As in the RME, the scheduler determines and allocates to a UE and an RB that have the highest PF metric and iterates the allocation consecutively to neighbors until another UE that has a higher metric value in the same RB is found. After the allocation procedure, the allocated UE (row) and RBs (columns) are excluded from the array, and the new PF metric for allocation adopting the *Tr* value is found among the remaining metrics. If the *Tr* value is 1, the allocation procedure is the same as in the RME allocation procedure. The scheduler performs the above procedure repeatedly and finally determines one allocation path that has the highest sum of metrics among the given *Tr* allocation paths. The IRME has the same algorithmic conditions as the RME, except for the *Tr* value [10]. In the appendix, we describe the complexity of the IRME algorithm.

Fig. 2 shows the examples of the RME and the IRME algorithm with a given 2-dimensioned array consisting of four UEs and seven RBs. We assume that the given metric values of the array are the same in the examples and that the *Tr* value is 2. After scheduling by the algorithms, the IRME with *Tr* =2 has a better result than the RME due to the consideration of one more resource allocation path. The RME algorithm is simple and yields better cell throughput (*i.e.*, the sum of the determined metric values for resource allocation) than a static scheduling algorithm such as round-robin scheduling. However, the RME does not scheduling in a flexible way, because the algorithm depends only on the metrics of the neighbor RBs. The IRME algorithm compensates this shortcoming of the RME, partly because the resource allocation paths are able to be considered dynamically by the given *Tr* value. However, a fixed *Tr* value is not flexible to respond quickly to the rapidly changing

numbers of UE. So this causes high complexity in the scheduling. In the next section, we propose a simple scheduling algorithm named MSCC that has the ability to overcome shortcomings of the RME and the IRME with low time complexity. We explain the MSCC with a flowchart and pseudo-code.

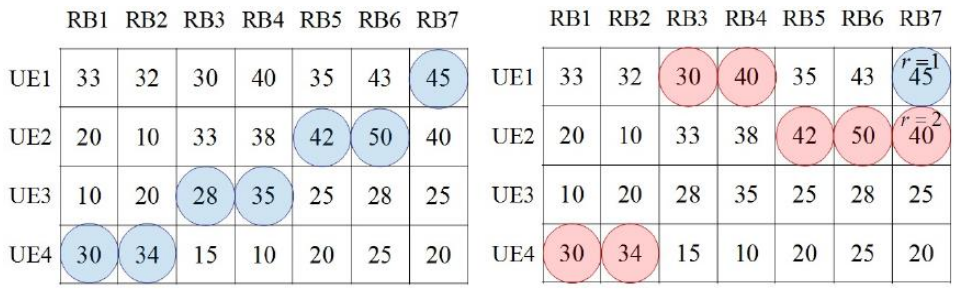

Conventional RME algorithm (50→42→45→35→28→34→30)

Improved RME algorithm (50→42→40→40→30→34→30)

Fig. 2. Examples of resource allocation.

3. PROPOSAL SCHEDULING ALGORITHM

In this section, we propose a scheduling scheme called maximum PF selection with the contiguity constraint (MSCC) that provides effective cell throughput with low complexity and improved fairness in SC-FDMA. The previous scheduling schemes depend on expansion to both sides of neighbor RBs after selecting the highest PF scheduling metric in a multi-dimensional array. However, these resource allocation schemes have some limitations in terms of scheduling flexibility and cause increased complexity in proportion to the number of the allocation paths considered. The MSCC is more flexible since it considers the allocation paths and attempts to improve the shortcomings of the previous algorithms. The MSCC finds the highest PF metrics, $m_{n,k}$, in each RB, whether it is available to be allocated or not in a descending order. Therefore the MSCC provides better performance than IRME, which uses the ranking threshold (*Tr*) value to search the resource allocation paths. We specifically describe the MSCC with a flowchart, pseudo-code, and the same example as in Fig. 2, in the following two subsections. We also analyze the complexity of the MSCC in the appendix.

3.1 Maximum PF Selection with Contiguity Constraint (MSCC)

Channel states (*i.e.*, SINR) generally have correlation with neighbor frequency bands and time slots, and the correlation in the frequency domain is not higher than that in the time domain (frequency selective fading). The previous schemes do not handle frequency selective fading effectively due to resource allocation depending on the expansion to both-sides of the neighbor's RB with the highest PF metric in the multi-dimensional array. The basic idea of the MSCC is that the scheduler preferentially finds the highest PF metrics of each RB to perform scheduling in an efficient way in any channel deviation while maintaining

the contiguity constraints. The MSCC's resource allocation aims at providing higher cell throughput, and dynamically considers according to the number of UEs or the drastic channel variation, which is different from the fixed *Tr* value of IRME. Fig. 3 shows specific step-by-step procedure in a flow chart for resource allocation in the MSCC.

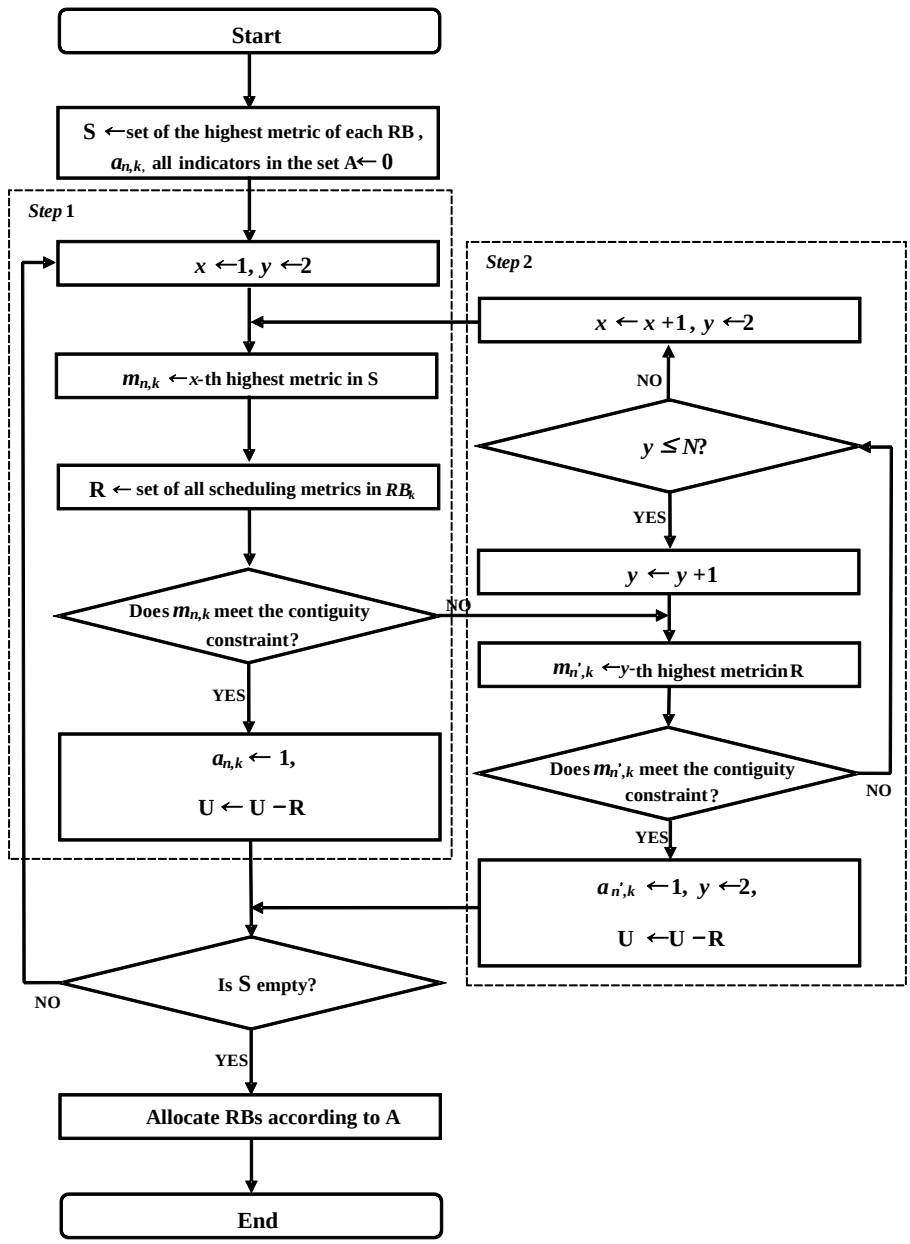

Fig. 3. Flowchart of the MSCC.

Given the input, the scheduler performs scheduling with all PF metrics until all RBs are allocated to all UEs as in the basic FDPS system of Section 2. Resource allocation procedure of MSCC has two steps after initialization. In the initialization, the scheduler creates a two-dimensional array (*i.e.*, set **U**) of UEs and RBs with the given PF metrics and determines the highest metric in each RB. The set **U** contains all scheduling metric values based on N UEs and K RBs, with the same meaning as the input matrix **M** in Section 2. Next, the scheduler searches for the highest PF scheduling metric value in RBs. Set **S** consists of the highest metrics in RBs. The chosen metric value is **denoted** as $m_{n,k}$, where n and k are the UE and RB to indicate the PF metric value, respectively ($1 \le n \le N$, $1 \le k \le K$). Set **A** contains indicators to indicate resource allocation status in the array, whose values are initialized to 0 with the same size of the set **U**.

***Step* 1:** The scheduler determines the highest PF metric value ($m_{n,k}$) and considers the contiguity constraint in set **S**. The contiguity constraint denotes that a UE's resource allocation should be the first time for the UE in the scheduling or should be consecutive with the allocated RBs. After deciding to allocate a PF metric as a resource, the scheduler changes the indicator ($a_{n,k}$) to 1, representing the resource allocation status in set **A**. The changed indicator value denotes that the RB is allocated to the UE corresponding to the indicator position. After the chosen PF metric value's indicator is changed in set **A**, the scheduler excludes all metrics associated with the allocated RB (*i.e.*, set **R**) in the array. Set **R** has all values in RB that has the chosen metric value and is used when the chosen value is not allocated. Whenever the scheduler decides the allocation, Set **S** newly consists of the rest of the values excluding the chosen value.

***Step* 2:** In the case where the chosen metric value is not allocated by the contiguity constraint, the scheduler tries to allocate values of other UEs (*i.e.*, one specific $m_{n,k}$, $1 \le n \le N$, $1 \le k \le K$) one-by-one in a descending order in the RB, including the chosen value. If the allocation is not finished after the scheduler considers all metrics that belong to the chosen RB, the scheduler postpones the allocation of the RB, including the chosen value, until the next time slot. It continues scheduling with the next highest value in the set S (*i.e.*, $x \leftarrow x+1$). The resource allocation for the postponed RB should be considered again, whenever the allocation of the current RB is decided. The postponed RB finally receives the RB allocation with a certain metric value, since the scheduling works until all RBs are allocated.

Fig. 4 shows the same example used to explain the RME and the IRME adopted by the MSCC. The scheduler determines the highest PF metric value in RBs at a given array. Then, **S** consists of {$m_{1,1}$ (=33), $m_{4,2}$ (=34), $m_{2,3}$ (=33), $m_{1,4}$ (=40), $m_{2,5}$ (=42), $m_{2,6}$ (=50), $m_{1,7}$ (=45)}, and the scheduler checks the contiguity constraint with the chosen values one-by-one in a descending order (*i.e.*, ***Step* 1**). In case of RB1 and RB4, the chosen PF metric values from **S** should not be allocated because of the allocated metric of RB7. The scheduler continues with the scheduling in ***Step* 2** when the chosen metric of **S** is impossible to allocate. In ***Step* 2**, the scheduler considers allocation again with metric values of **R** excluding the highest metric. Therefore **Rs** of RB1 and RB4 do not include the highest metric and consist of {$m_{4,1}$ (=30), $m_{2,1}$ (=20), $m_{3,1}$ (=10)} and {$m_{2,4}$ (=38), $m_{3,4}$ (=35), $m_{4,4}$ (=10)}, respectively.

The dotted circle denotes that the PF metric is selected as the highest metric value in

the RB but is excluded due to the contiguity constraint. Scheduling the example as in the flowchart, we find out the sum of the MSCC (274) is higher than other sums of the RME (264) or the IRME (266), because the MSCC preferentially allocates the highest values in each RB, rather than scheduling resource allocation based on expansion from the highest metric to both-side neighbors. In the example of Fig. 4, the MSCC does not provide resource allocation to UE3. However, the UE3 has chance to acquire more resources than other UEs at next scheduling through the PF metric processing, and thus the MSCC algorithm guarantees data fairness. Conclusively, the MSCC algorithm performs more flexible scheduling because it considers resource allocation more dynamically every time than the fixed ranking threshold of IRME in various environments that can experience drastic changes in the number of UEs or channel states.

	RB1	RB2	RB3	RB4	RB5	RB6	RB7
UE1	33	32	30	40	35	43	45
UE2	20	10	33	38	42	50	40
UE3	10	20	28	35	25	28	25
UE4	30	34	15	10	20	25	20

Fig. 4. Examples of resource allocation by the MSCC (50→45→42→38→34→33→30).

3.2 Pseudo-code of the MSCC Algorithm

Table 1 and table 2 show the MSCC pseudo-code. Table 2 describes the initialization step of **A** and **S** for the MSCC scheduling. The pseudo-code has the same procedures and notation as in the flowchart used to introduce the MSCC earlier. The scheduling continues performing until resource allocations of all RBs are completed after considering the highest metric values in each RB. It means scheduling repetition until all the constituent metric values are excluded in set **S** (*i.e.*, ***Step* 1**). The scheduler considers the chosen PF metric value with the contiguity constraint. If the chosen value does not meet the contiguity constraint, other values in the same RB are considered in descending order using variable *y* (*i.e.*, ***Step* 2**). If all metric values do not meet the constraint, the scheduler increases variable *x* and goes on with the scheduling with the next highest PF metric value in set **S** (*i.e.*, in case variable *y* exceeds *N* in ***Step* 2**). The scheduler considers the postponed PF metric value with contiguity constraint again in the updated array, after resource allocation of the new chosen metric is completed.

The MSCC schedules in the two-dimension array consisting of PF scheduling metric values. The metric values are calculated based on channel states for each UE and HARQ (hybrid automatic retransmit request) information used for the UE that requires retransmission. The MSCC performs scheduling with the highest PF metric values in each RB, while the RME and the IRME perform based on expansion to neighbor RBs. As a result, the scheme has the benefit that it easily handles sharp changes in channel

gain (*i.e.*, sudden drop) that may occur with all UEs. The MSCC performs flexible allocation, even with sharp deviations in channel states and the number of UEs, because it performs dynamic scheduling for every input array, unlike the IRME, which has a static input parameter (*i.e.*, ranking threshold). The MSCC is also better than the two previous schemes in terms of time complexity due to scheduling based on an array consisting of the highest metric values in each RB.

Table 1. Pseudo-code of the MSCC.

MSCC Scheduling Procedure

Input: set **U** consisted with all PF metrics $m_{n,k}$ ($1 \le n \le N, 1 \le k \le K$)

Output: set **A** consisted with all indicators $a_{n,k}$ with either 0 or 1

($1 \le n \le N, 1 \le k \le K$)

Procedure: *MSCC*(**U**, **A**)

$x \leftarrow 1, y \leftarrow 2$

Initialize input parameters *initialization*(**U**, **A**, **S**)

while (**S** $\neq \emptyset$) **do** // ***Step 1***

  $m_{n,k} \leftarrow x$-th highest metric in the set **S**

  Let the set **R** be the set of all scheduling metrics in the k-th RB

  if ($m_{n,k}$ is the first RB assigned to user n) or

  ($m_{n,k}$ is adjacent to RB assigned to user n) **then**

    $a_{n,k} \leftarrow 1$, **U** $\leftarrow$ **U** – **R**, **S** $\leftarrow$ **S** –$\{m_{n,k}\}$

    $x \leftarrow 1$

  Else

    $x \leftarrow x + 1, y \leftarrow 2$

    while ($y \le N$) **do** // ***Step 2***

      $m_{n',k} \leftarrow y$-th highest metric in the set **R**

      if ($m_{n',k}$ is adjacent to RB assigned to user n') **then**

        $a_{n',k} \leftarrow 1$, **U** $\leftarrow$ **U** – **R**, **S** $\leftarrow$ **S** –$\{m_{n,k}\}$

16:	$x \leftarrow 1$, y $\leftarrow 2$
17:	**Break**
18:	**Else**
19:	$y \leftarrow y+1$

Table 2. Initialization part.

Initialization Procedure

Input: set **U** consisted with all PF metrics $m_{n,k}$ ($1 \le n \le N, 1 \le k \le K$)

Output: set **A** consisted with all indicators $a_{n,k}$ with either 0 or 1

($1 \le n \le N, 1 \le k \le K$)

:set **S** consisted with the highest PF metrc in each RB

($1 \le n \le N, 1 \le k \le K$)

Procedure: *initialization*(**U**, **A**, **S**)

1: $n \leftarrow 0, k \leftarrow 0$

2: **for** (n =1; $k \le N$; n++;) // ***Initialization*** **A**

3: **for** (k =1; $k \le K$; k++;)

4: $a_{n,k} \leftarrow 0$, **A** $\cup \{a_{n,k}\}$

5: **for** (k =1; $k \le K$; k++;) // ***Initialization*** **S**

6: **for** (n =1; $n \le N$; n++;)

7: **if** ($m_{n,k}$ is the highest PF metric in the k-th RB)

8: **S** $\cup \{m_{n,k}\}$

9: **Break**

4. PERFORMANCE EVALUATION

In this section, we analyze the simulation results of RME, IRME, and the proposed

MSCC scheduling algorithm. We simulated them in terms of fairness, throughputs, and PAPR, explain the parameters used for the simulation, and show the simulation results.

4.1 Simulation Environments

We performed a system-level simulation of SC-FDMA based on the 3GPP LTE system model to analyze fairness and throughput of the MSCC with those of previous schemes.

For the performance evaluation, we measure a performance in a single-cell environment where no cell interferes with its neighbor. Table 3 describes simulation parameters based on the typical urban channel model [18-21]. In this paper, we use the MCS table instead of Shannon capacity to analyze practical results [22]. We use the proportionally fair (PF) method as the scheduling metric. The PF method is represented by (3) to guarantee a certain level of fairness regardless of algorithms. Here $r_{i,j}(t)$ denotes a data rate of the j-th RB that could be allocated to UE i at time t. $R_i(t)$ denotes an accumulated data rate of RB that is allocated to UE i until time t. An UE that relatively unfairly receives resources at time t has a chance to receive more resource allocation in the next time slot using PF as a scheduling metric.

Table 3. Simulation Parameters.

Parameters	Values
System bandwidth	20 MHz
Used subcarriers	1200
FFT size	2048
Subcarrier spacing	15 kHz
RB size	12 subcarriers
RB bandwidth	180 kHz
Number of RBs	100
Cell radius	500m
UE power	23dBm
User distribution	Uniform
User speed	3km/h, 300km/h
Traffic model	Full buffer
Transmission time interval (TTI)	1 ms
Channel model	Typical Urban
Power control	No
Number of active users in cell	10, 20, 30, 40, 50, 60, 70, 80, 90, 100
User receiver	1x2/MMSE
Access scheme	SC-FDMA
Scheduling metric	Proportional fair
Scheduling algorithms	RME, IRME, MSCC
Available MCSs	QPSK: 1/3, 1/2, 2/3. 3/4 16QAM: 1/2, 2/3, 3/4 64QAM: 1/2, 2/3, 3/4, 5/6

$$m_{i,j} = \frac{r_{i,j}(t)}{R_i(t)} \tag{3}$$

In equation (4), Jain's fairness index is used for fairness evaluation. $R_i(\Delta t)$ represents a real data transmission rate of i for time interval Δt, where N represents the number of users in the system.

$$\text{fairness} = \frac{\left[\sum_{i=1}^{N} R_i(\Delta t)\right]^2}{\left[N \cdot \sum_{i=1}^{N} R_i(\Delta t)^2\right]} \tag{4}$$

4.2 Simulation Results

Fig. 5 describes the changes of fairness according to the number of users moving at the speed of 3km/h. In general, as the number of users increases, fairness diminishes, irrespective of the schemes; the number of RBs allocated to each user decreases and the choices to consider resources are reduced. The three schemes adopt the PF method for scheduling metric values, so a certain level of fairness can be guaranteed. The IRME scheme enhances throughput compared to the RME, so it has lower fairness generally than the RME. The MSCC scheme guarantees a similar fairness with RME. The MSCC has up to 10% and 3% higher fairness than the IRME and the RME, respectively, for between 40 and 80 users. This result shows that the MSCC has the best fairness among these scheduling algorithms. The reason is that the PF scheduling metric is more effectively used in the scheme because of scheduling resource allocation in each RB.

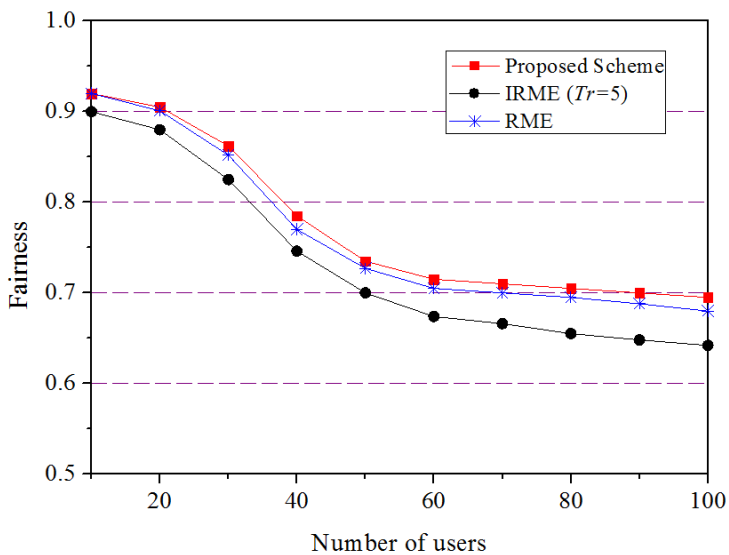

Fig. 5. Fairness value according to number of users.

Fig. 6 describes the changes of system throughput according to the number of users. The users move at the speed of 3km/h. For all three schemes, throughputs increase gradually as the number of users increases, but these are saturated at certain levels. The saturation is due to the throughputs being close to limitation as many as users. The system throughput increases, regardless of schemes, as the number of users increases, because resources can be allocated to users who have better performance as the number of users increases. This is defined as the multi-user diversity gain. Fig. 6 shows that the MSCC has the best system throughput in all regions excluding the number of users less than 10, with gaps of up to 12% and 16% compared to that of the IRME and RME, respectively. For the number of users less than 10, the IRME has better result but the difference, 1%, is fairly marginal. The IRME has a higher throughput than the RME in all ranges up to 100 users, and shows a gap of up to 17% in the region between 10 users and 20 users. This is because it has more flexible scheduling compared to the RME thanks to the ranking threshold. The MSCC has higher throughput than that of IRME up to 100 users.

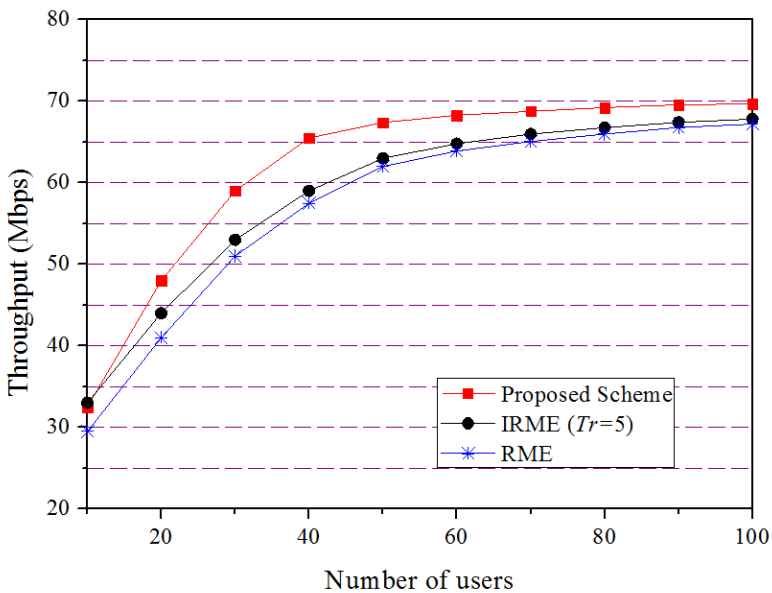

Fig. 6. System throughput according to number of users (3km/h user speed).

Fig. 7 describes the changes of system throughput according to the number of users who have 300km/h speed. Similar to Fig. 6, in all three schemes, throughput increases gradually as the number of users increases, and is saturated at a certain level. However, these total system throughputs show about 30% lower results than those in Fig. 6 because of extremely different speed of users. The cause is defined as a fast fading environment. In the fast fading environment, channel states rapidly fluctuate in every TTI and thus the users have limited channel quality with uplink RB allocation constraint. Therefore the three schemes, which are seriously affected by channel quality, have no great differences in Fig. 7. Despite the limitation, the MSCC has the better system throughput in the re-

gions from 40 to 100 users than IRME and RME. The IRME scheme is mainly focused on the improvement of the system throughput and shows a slightly better performance for the number of users less than 40. However, in Fig. 7 similar to Fig. 6, the IRME is not better than the MSCC in the condition which maximizes multi-user diversity gain (i.e., over 40 users). The RME has the lowest system throughput even in the fast fading environment. As a result, the MSCC generally provides the best results among the three schemes performance evaluated.

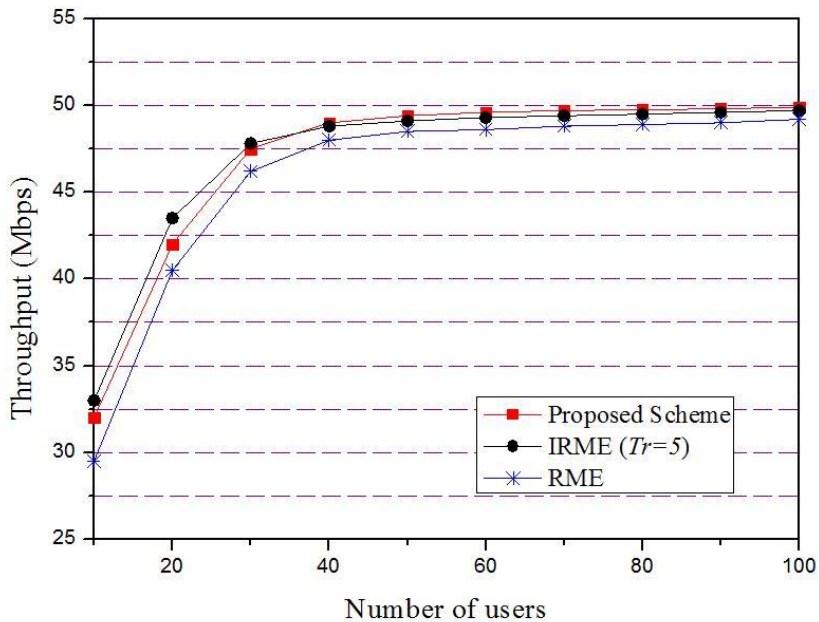

Fig. 7. System throughput according to number of users (300km/h user speed).

Fig. 8 shows the Cumulative Distribution Function (CDF) result of cell edge user throughput with 20 users. The users move at the speed of 3km/h. The cell edge user throughput means the result of the lowest 5% user throughput among cell users. IRME scheme has about 190kbps as average user throughput, and this is the worst performance. This means that a cell edge user's resource allocation is not considered well because the IRME uses a ranking threshold that chooses the allocation path considered system throughput. In other words, a user who received resources rarely at a previous time does not have much recovery because of the tanking threshold, even though the user keeps having a chance to use more resources. The RME has about 300kbps of average user throughput. The RME achieves the best edge user throughput among three schemes and satisfies data requirements of the cell edge users well, unlike the system throughput result of Fig. 6. The MSCC has about 240kbps of average user throughput, which is lower than that of the RME but higher than that of the IRME. Consequently, the MSCC is the best scheme in terms of total system throughput, and the RME is a superior scheme to the

others. The MSCC comes in second with performance similar to the RME in terms of cell edge user throughput.

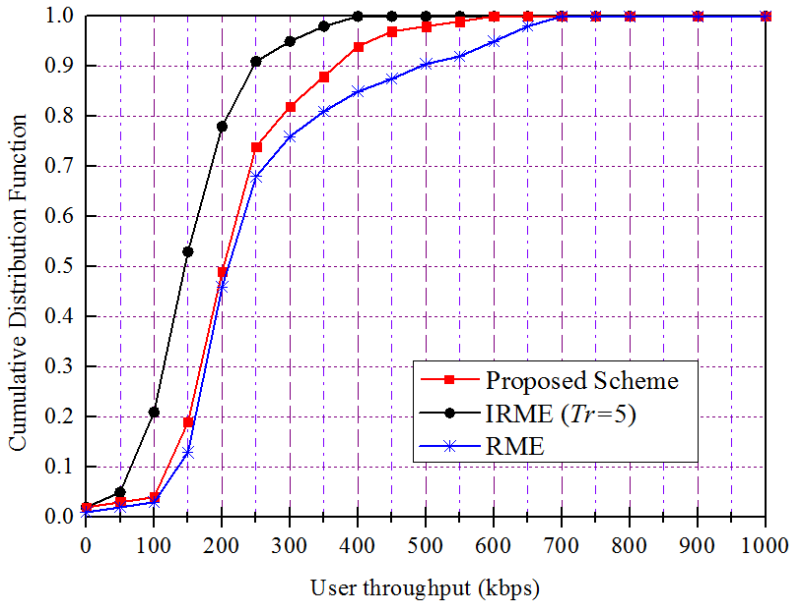

Fig. 8. Edge user throughput (20 users).

Fig. 9 shows the result of average edge user throughput according to the number of users. The users move at the speed of 3km/h. As we described system throughput in Fig. 6, average cell edge user throughput also increases gradually as the number of users increases because users who have better channel conditions have more chances to receive resources, as many as the increase in number of users. Among the three schemes, the RME has the best performance and increases user throughput gradually from about 250kbps for 10 users to about 760kbps for 100 users. IRME has the worst performance which increases user throughput gradually from about 160kbps for 10 users to about 650kbps for 100 users. The proposed MSCC also increases user throughput gradually from about 220kbps for 10 users to about 720kbps for 100 users. The MSCC has lower user throughput up to 18% compared to RME but has higher user throughput up to 14% compared to IRME. Nevertheless, all of three schemes have small differences within about 100kbps.

Fig. 10 shows the PAPR result of three schemes. The PAPR of SC-FDMA generally is lower than 10dB [4-6], because it commonly has lower PAPR than OFDMA due to the single-carrier characteristic. The MSCC and previous algorithms are shown to similar PAPR results from about 8.5 dB to about 9.5dB. Overall, the RME has the best result, but is similar to that of the MSCC. The IRME scheme has the highest total PAPR result, and it is about 4.5% higher than the MSCC. The MSCC has better PAPR than IRME but not better than RME. However, all three schemes have no problems for adoption in LTE uplinks because the schemes satisfy a certain level of PAPR which has the characteristic of SC-FDMA.

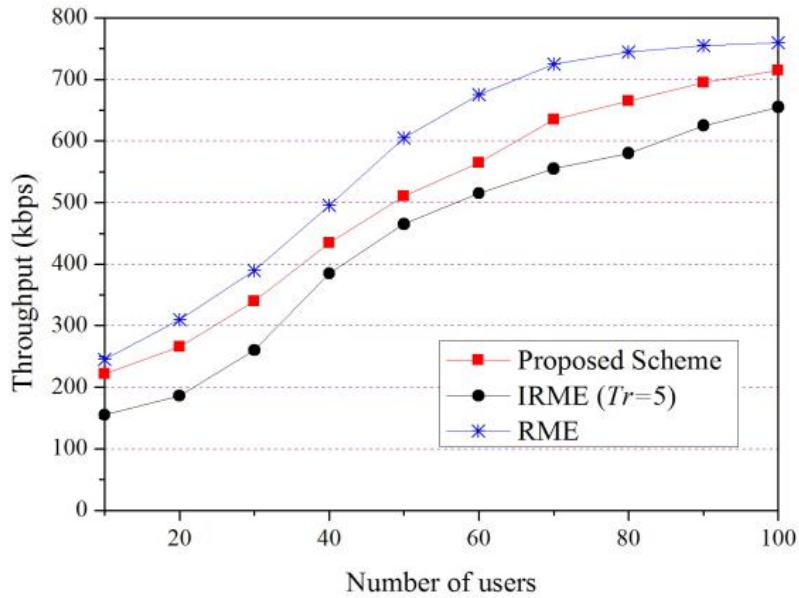

Fig. 9. Low 5% user throughput according to number of users.

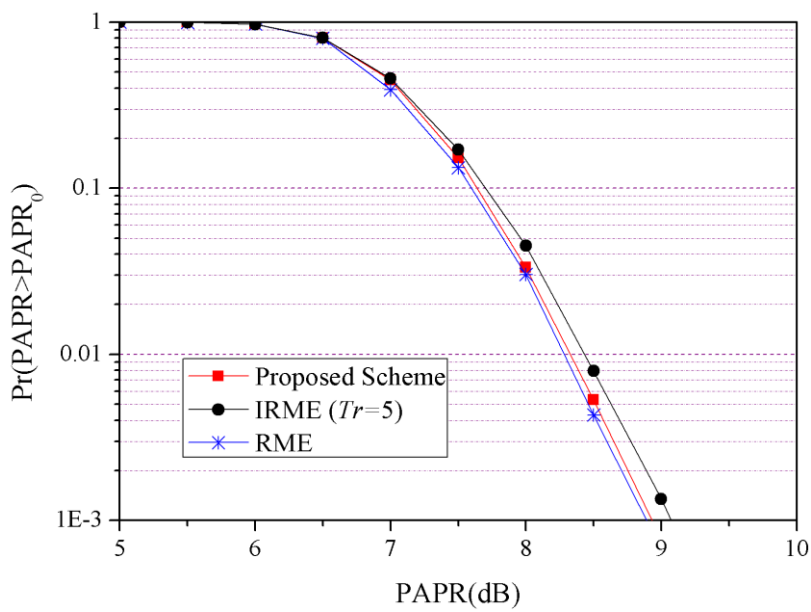

Fig. 10. CCDF results according to scheduling algorithms.

5. CONCLUSION

In this paper, we propose MSCC, a FDPS algorithm applied to SC-FDMA for low PAPR in the LTE uplink. The suggested the MSCC satisfies contiguity constraint on resources of SC-FDMA, guarantees high cell throughput and fairness, and has low-complexity scheduling. We compared the performance of MSCC algorithm to the RME and the IRME algorithms using a PF metric as a scheduling metric. We verified that it has a high throughput in most regions simulated. In addition, the time complexity of the MSCC, through the asymptotic notation, always lower than the previous two algorithms based on the environment of LTE mobile communication. The throughput of the MSCC is superior to that of the others, because it operates scheduling based on the highest metrics in each RB, rather than a resource allocation by expansion to the neighbor RBs. Therefore, the MSCC provides an improved scheduling feature compared to other algorithms in a frequency-selective fading environment in which a gain can suddenly change in one UE channel state.

REFERENCES

1. Zhang. X. P. and Ryu. H-G, "ICI problem and compensation in MIMO SC-FDMA system with SC-SFBC scheme," *International Journal of Communication Systems*, 2010; 23(12):15211536.
2. 3GPP TR 25.814. V7.1.0, *Physical Layer Aspects for Evolved UTRA*, Sep. 2006.
3. Good. R., Gouveia, F. C, Ventura. N, and Magedanz, T, "Session-based end-to-end policy control in 3GPP evolved packet system," *International Journal of Communication Systems*, 2010; 23:861–883. DOI: 10.1002/dac.1096.
4. Myung. H.G, Lim. J, Goodman. D.J, "Single carrier FDMA for uplink wireless transmission," *IEEE Vehicular Technology Magazine*, 2006; 30-38.
5. Myung. H.G, Lim. J, Goodman. D.J, "Peak-To-Average Power Ratio of Single Carrier FDMA Signals with Pulse Shaping," *IEEE Proc. of the PIMRC*, 2006; 1-5.
6. Berardinelli. G, Ruiz. T, Frattasi. S, Rahman. M, and Mogensen. P, "OFDMA vs. SC-FDMA: Performance Comparison in Local Area IMT-A Scenarios," *IEEE Wireless Communications*, 2008; 64-73.
7. Lim. J, Myung. H.G, and Goodman. D.J, "Proportional Fair Scheduling of Uplink Single-Carrier FDMA Sys-tems," *IEEE Proc. of the PIMRC*, 2006.
8. Temino. L, Berardinelli. G, Fattasi. S, and Mogensen. P, "Channel-Aware Scheduling Algorithms for SC-FDMA in LTE Uplink," *IEEE Proc. of the PIMRC*, 2008.
9. Safa. H, and Tohme. Kamal, "LTE uplink scheduling algorithms: Performance and challenges," *IEEE Proc. of the ICT*, 2012.
10. Liu. F, She. X. Chen. L, and Otsuka. H, "Improved Recursive Maximum Expansion Scheduling Algorithms for Uplink Single Carrier FDMA System," *IEEE Proc. of the VTC Spring*, 2010.
11. Calabrese. F.D, Michaelsen. P. H, Rosa. C, Anas. M, and Castellanos. C.U, "Search-Tree Based Uplink Channel Aware Packet Scheduling for UTRAN LTE," *IEEE Proc. of the VTC*, 2008; 1-5.
12. Wengerter. C, Ohlhorst. J, and Elbert. A.G.E.V, "Fairness and Throughput Analysis

for Generated Propor-tional Fair Frequency Scheduling in OFDMA," *IEEE Proc. of the VTC spring*, 2005.
13. Suk-Bok. L, Pefkianakis. I, Meyerson. A, Shugong. X, Songwu. L, "Proportional Fair Frequency-Domain Packet Scheduling for 3GPP LTE Uplink," *IEEE Proc. of the INFOCOM*, 2009; 2611-2615.
14. Sunay. M.O, and Eksim. A, "Fair scheduling for spectrally efficient multi-service data provisioning," *International Journal of Communication Systems*, 2004; Vol. 167, pp.615-642, August.
15. Wengerter. C, Ohlhorst. J, and Elbert. A.G.E, "Fairness and Throughput Analysis for Generalized Propor-tional Fair Frequency Scheduling in OFDMA," *IEEE Proc. of the VTC spring*, 2005.
16. Pokhariyal. A, Monghal. G, Pederson. K. I., Mogensen. P. E., Kovacs. I. Z., Rosa. C, and Kolding. T. E, "Frequency Domain Packet Scheduling Under Fractional Load for the UTRAN LTE Downlink," *IEEE Proc. of the VTC spring*, 2007.
17. Calabres. F. D, Anas. M, Rosa. C, Mogensen. P. E, and Pedersen. K. I, "Performance of a Radio Resource Al-location Algorithm for UTRAN LTE Uplink," *IEEE Proc. of the VTC spring*, 2007.
18. 3GPP TR 25.943, Technical Specification Group Radio Access Networks– Deployment Aspects, 2009.
19. 3GPP TS 36.300 V10.11.0, *E-UTRA and E-UTRAN Overall Description*, Sep. 2013.
20. 3GPP TS 36.201 V10.0.0, *E-UTRA LTE Physical Layer-General Description*, Dec. 2010.
21. Dinis. R, Falconer. D, Lam. C.T, and Sabbaghian. M, "A Multiple Access Scheme for the Uplink of Broadband Wireless Systems," *IEEE Proc. of the GLOBECOM*, 2004.
22. 3GPP TR 36.942 V10.3.0, *Radio Frequency (RF) System Scenarios*, Jul. 2012.
23. 3GPP TS 36.211 V10.7.0, *Physical Channels and Networking*, Mar. 2013.
24. Li. L, Wu. G, Xu. H, Li. G.Y, and Feng. X, "A Practical Resource Allocation Approach for Interference Management in LTE Uplink Transmission" *Journal of Communications*, 2011; 6(4): 301-305.

APPENDIX

In this section, we analyze the time complexity of the RME, the IRME, and the proposed scheme. We assume that there are N UEs and K RBs, and the scheduling of each scheme always performs in the worst case. We calculated the final complexity of each scheme with two cases that are $N > K$ and $K > N$.

***RME Algorithm*:** The RME tries to allocate resources to neighbor RBs located on both sides, with the highest PF metric value in a given two-dimensional array. We assume that there is no expansion to neighbor RBs as the worst case in RME scheduling. The case of $N > K$ means that the number of UEs is higher than the number of RBs. The complexity of RME requires the sum from NK to be $(N-(K-1))\times(K-(K-1))$ for searching the first scheduling metric value, because this algorithm performs until $K=1$. Equation (5) and equation (6) are shown this step. Then, this complexity is organized into $O(NK^2)$ via equation (6) with arithmetical and geometric progression, and equation (7)

shows the calculation process of equation (6). Conversely, when $K > N$, the complexity requires the sum from NK to be $(N-(N-1))\cdot(K-(N-1))$, and equation (8) and equation (9) show calculation processes. The equation (9) is calculated similarly to equation (6), and $O(N^2K)$ is the organized complexity in the case of $K > N$. The final complexity is $O(NK(N+K))$, considering both of the cases.

$$O\left(N\times K+(N-1)\times(K-1)+(N-2)\times(K-2)+...+(N-(N-1))\times(K-(N-1))\right) \quad (5)$$

$$O\left((N)NK-\sum_{i=1}^{N-1} i\cdot K-\sum_{i=1}^{N-1} i\cdot N+\sum_{k=1}^{N-1} k^2\right) \quad (6)$$

$$O\left(N^2K-\frac{(N-1)N}{2}K-\frac{(N-1)N}{2}N+\frac{N(N-1)(2N-1)}{6}\right) \quad (7)$$

$$O(N\times K+(N-1)\times(K-1)+(N-2)\times(K-2)+...+(N-(K-1))\times(K-(K-1))) \quad (8)$$

$$O\left((K)NK-\sum_{i=1}^{K-1} i\times N-\sum_{i=1}^{K-1} i\times K+\sum_{x=1}^{K-1} x^2\right) \quad (9)$$

$$O\left(NK^2-\frac{(K-1)K}{2}K-\frac{(K-1)K}{2}N+\frac{K(K-1)(2K-1)}{6}\right) \quad (10)$$

***IRME Algorithm*:** In the IRME, the ranking threshold is additionally needed to provide more flexible scheduling in terms of throughput from the same condition with RME. The threshold value is statically provided to the scheduler as an input parameter before performing scheduling. Therefore, the worst case to schedule the IRME is that the ranking threshold is adopted to be as many as the number of UEs, and the scheduler performs scheduling with this threshold value. In the case of $N > K$, the complexity of the IRME is organized from equation (11) into $O(N^2K^2)$, because the complexity incurs a time cost to the sum of the ranking threshold and the RME. Inversely, for $K > N$, the complexity requires equation (12) and is organized into $O(N^3K)$. The final complexity of IRME is calculated as $O(N^2K(N+K))$, considering both of the cases.

Table 4. Complexity results.

	Complexity
RME	$O(NK(N+K))$
IRME	$O(N^2K(N+K))$
MSCC	$O(NK\log_2 N+K\log_2 K)$

$$O(N)\times O(N^2K) \tag{11}$$

$$O(N)\times O(NK^2) \tag{12}$$

***MSCC Algorithm*:** The MSCC performs scheduling based on the highest metrics in each RB in the input two-dimensional array. We assume the worst case in algorithm performance of the MSCC in which no chosen highest metric values satisfy the contiguity constraint, and the scheduler should consider all the other metric values in the RB that has the chosen metric value. First, the necessary complexity is $O(NK\log_2 N)$ to perform binary search with all metric values to search for the highest PF metric values in each RB. The complexity is also needed, as much as $O(K\log_2 K)$, due to the arrangement in descending order. The complexity $O(NK)$ is also needed to consider all metric values in the RB that have the chosen metric value with the contiguity constraint. In the case where $N > K$, the complexity is organized from equation (13) into $O(NK\log_2 N)$. In case where $K > N$, the complexity is organized by equation (14). Therefore, the final complexity of MSCC is $O(NK\log_2 N)$, considering both cases. If the complexity is considered in an environment that has an extremely low value among UE or RB, the result could differ. However, the MSCC always has the lowest complexity cost of the three schemes in the current mobile communication environment. Table 4 summarizes the final complexity of each scheme.

$$O(NK\log_2 N + K\log_2 K + NK) \tag{13}$$

$$O(NK\log_2 N + K\log_2 K) \tag{14}$$

Hongsuk Kim received the B.S degree in Korea Maritime University and received the M.S. degree in Information and Communication Engineering from Sungkyunkwan University, Korea, in 2012. He is currently working at LG Electronics. His research interests include long term evolution, long term evolution advanced, and resource allocation.

Mihui Kim received the B.S. and M.S. degrees in Computer Science and Engineering from Ewha Womans University, Korea, in 1997 and 1999, respectively. During 1999–2003, she stayed in Switching & Transmission Technology Lab., Electronics and Telecommunications Research Institute (ETRI) of Korea to develop MPLS System and the 10Gbps Ethernet System. She also received the Ph.D. degree in Ewha Womans University in 2007. She was a postdoctoral researcher of the

department of Computer & Web Information Engineering, Computer System Institute, North Carolina State University from 2009 to 2010. She is currently an assistant professor of the department of computer engineering, Hankyong National University Anseong-si, Gyeonggi-do in Republic of Korea. Her research interests include design of efficient network protocols, and mobile/sensor/smart grid/cognitive network security.

Min Young Chung received the B.S., M.S., and Ph.D. degrees in electrical engineering from the Korea Advanced Institute of Science and Technology, Daejeon, Korea, in 1990, 1993, and 1999, respectively. From January 1999 to February 2002, he was a Senior Member of Technical Staff with Electronics and Telecommunications Research Institute, where he was engaged in research on the development of multiprotocol label switching systems. In March 2002, he joined the Faculty of Sungkyunkwan University, Suwon, Korea, where he is currently a Professor with the College of Information and Communication Engineering. His research interests include Internet and routing, mobile IP, wireless communication networks, wireless LAN/PAN, and next-generation wireless communication networks. He worked as an editor on the Journal of Communications and Networks from January 2005 to February 2011, and is a member of ACM, IEEE, IEICE, KICS, KIPS, and KISS.

Tae-Jin Lee received his B.S. and M.S. in electronics engineering from Yonsei University, Korea in 1989 and 1991, respectively, and the M.S.E. degree in electrical engineering and computer science from University of Michigan, Ann Arbor, in 1995. He received the Ph.D. degree in electrical and computer engineering from the University of Texas, Austin, in May 1999. In 1999, he joined Corporate R & D Center, Samsung Electronics where he was a senior engineer. Since 2001, he has been an Professor in the School of Information and Communication Engineering at Sungkyunkwan University, Korea. He was a visiting professor in Pennsylvania State University from 2007 to 2008. His research interests include performance evaluation, resource allocation, Medium Access Control (MAC), and design of communication networks and systems, wireless MAN/LAN/PAN, ad-hoc/sensor/RFID networks, next generation wireless communication systems, and optical networks. He has been a voting member of IEEE 802.11 WLAN Working Group, and is a member of IEEE and IEICE.

Hyunseung Choo received the B.S. degree in mathematics from Sungkyunkwan University, Korea in 1988, the M.S. degree in computer science from the University of Texas at Dallas, USA in 1990, and the Ph.D. degree in computer science from the University of Texas at Arlington, USA in 1996. From 1997 to 1998, he was a Patent Examiner at Korean Industrial Property Office. Since 1998, he has joined the College of Information and Communication Engineering, Sungkyunkwan University, and is an Associate Professor and Director of Convergence Research Institute. Since 2005, Dr. Choo is Director of Intelligent HCI Convergence Research Center (eight-year research program) supported by the Ministry of Knowledge Economy (Korea) under the Information Technology Research Center support program supervised by the Institute of Information Technology Assessment. His research interests include wired/wireless/optical embedded networking, mobile computing, and grid computing. He is Vice President of Korean Society for Internet Information (KSII). Dr. Choo has been Editor-in-Chief of the Journal of KSII for three years and journal editors of Journal of Communications and Networks, ACM Transactions on Internet Technology, International Journal of Mobile Communication, Springer-Verlag Transactions on Computational Science Journal, and Editor of KSII Transactions on Internet and Information Systems since 2006. He has published over 200 papers in international journals and refereed conferences. Dr. Choo is a member of IEEE and ACM.